

On the Helium fingers in the intracluster medium

Shubhadeep Sadhukhan^{1*}, Himanshu Gupta^{1†}, and Sagar Chakraborty^{1‡}

¹ *Department of Physics, Indian Institute of Technology Kanpur, U.P.-208016, India.*

26 March 2024

ABSTRACT

The primary goal of this paper is to build upon the machinery usually employed to study the salt finger instability in order to address the onset of the similar double diffusive convection phenomenon in the intracluster medium — the weakly-collisional magnetized inhomogeneous plasma permeating galaxy clusters; and subsequently, to investigate the nature of the width of the analogous Helium fingers in the supercritical regime of the instability. Specifically, we conclude that the width of the Helium fingers scales as one-fourth power of the radius of the inner region of the ICM. In the process, we also find out the explicit mathematical expression of the criterion for the onset of the heat-flux-driven buoyancy instability modified by the presence of inhomogeneously distributed Helium ions in the galaxy cluster. This criterion incorporates the contribution of the magnetic tension into it.

Key words: galaxies: clusters: intracluster medium - instabilities - magnetohydrodynamics (MHD).

1 INTRODUCTION

The intracluster medium (ICM) that permeates galaxy clusters is a weakly collisional, high-beta, multi-species plasma (Carilli & Taylor 2002; Peterson & Fabian 2006). Owing to the presence of the magnetic field, the transports of the heat and the momentum, and the diffusion of ions are anisotropic in the ICM. Straightforward linear stability analysis establishes that convection ensues in the ICM — assumed homogeneous and initially at rest — due to the onset of either the magnetothermal instability (MTI) (Balbus 2000, 2001) or the heat-flux-driven buoyancy instability (HBI) (Quataert 2008).

Since the ICM is composed of mainly electrons, Hydrogen ions, Helium ions and a very small fraction of heavier elements, it is intuitive, and theoretically proposed, that the different ions would diffuse to enrich (Fabian & Pringle 1977; Rephaeli 1978; Abramopoulos et al. 1981; Qin & Wu 2000; Chuzhoy & Nusser 2003; Chuzhoy & Loeb 2004) the cluster core with heavy elements along with Helium ions. Moreover, since both Hydrogen and Helium in the ICM are fully ionized rendering measurement of their abundances using traditional spectroscopic techniques difficult, there is no full-proof justification that the elements are homogeneously mixed. However, the theoretical investigations, with probably Pessah & Chakraborty (2013); Berlok & Pessah (2015, 2016) as exceptions, of convective instabilities in the ICM mostly consider it as a homogeneous medium for simplicity. This is rather unsatisfactory. In fact it has been argued that during the diffusion

process a nonzero gradient of mean molecular weight is created in the ICM (Qin & Wu 2000; Peng & Nagai 2009; Shtykovski & Gilfanov 2010; Bulbul et al. 2011) and it has non-trivial effects on the HBI and the MTI (Pessah & Chakraborty 2013). Thus, in spite of its simplicity, the assumption of a homogeneous medium must be dropped in order to understand the interplay between the process of Helium sedimentation and the convective instability arising out of inhomogeneity thus created.

As done in this paper, in the first approximation, one may ignore the far rarer heavier ions and consider the plasma as a dilute binary mixture of Hydrogen and Helium ions (and, of course, electrons). The nature of Helium sedimentation — a very important phenomenon in itself — on to the cluster core may affect different physical quantities such as the total mass of the cluster (Qin & Wu 2000), cosmological parameters from the observational data (Markevitch & Vikhlinin 2007; Peng & Nagai 2009); and thus may need to be considered for more precise calculations (Mroczkowski 2011; Bulbul et al. 2011) of the cluster mass and the Helium abundance profile in the cluster core as determined from observational X-ray data.

This simultaneous presence of the temperature and the composition gradients is reminiscent of familiar earthly situations conducive to the common double diffusive instabilities found in the oceans where vertical gradients of temperature and salinity are found naturally. In the gravitationally stably stratified case where hot salty water is put on top of cold fresh water, salt-fingers are observed (Stern 1960) because of the difference in the diffusivities of salt and heat — salt diffuses relatively slower. Stability analyses (Stern 1960; Schmitt 1979) establish that the salt-fingers are observed in the supercritical regime well beyond the scope of the linear stability analysis. More elaborate treatment of the double

* Email: deep@iitk.ac.in

† Email: hiugupta@iitk.ac.in

‡ Email: sagarc@iitk.ac.in

diffusive convection is considered in many papers (Monchick & Mason 1967; McDougall 1981a; Kunze 1987; McDougall 1981b; Özgökmen et al. 1998; Radko 2008, 2010). It interests us to note that double diffusive convection has been invoked in the astrophysical contexts to investigate convection in stellar interiors (Ulrich 1972), photospheric composition of low mass giants (Charbonnel & Zahn 2007b), and galactic evolution of ^3He (Charbonnel & Zahn 2007a).

In view of the above we envisage, in the context of the ICM, the existence and the importance of an instability analogous to the salt finger instability. Therefore, we extend the study of double diffusive convection to the situations of astrophysical interest in which the plasma is only weakly-collisional (meaning that the mean free path for particles to interact is much larger than the Larmor radius) and in which transport properties are anisotropic with respect to the direction of the magnetic field. In the inner region of the galaxy cluster where the temperature increases with the distance from the core of the galaxy cluster (Vikhlinin et al. 2006), the mean molecular weight (or equivalently concentration of Helium) is also predicted (Bulbul et al. 2011) to have a positive gradient. Consequently, we expect formation of fingers (analogous to the salt fingers in some geophysical contexts) in the supercritical regime of the convective instability. We would call such columnar structures, effecting radial mixing of the ICM, Helium fingers for obvious reasons: in these fingers concentration of Helium is relatively higher. In this paper, we investigate how the width of the Helium fingers scale with the system parameters and find for it a power law behaviour w.r.t. the gradients of the temperature and the mean molecular weight.

2 THE MODEL SYSTEM

The inherent nonlinear nature of the governing dynamical equations, along with the complicated boundary conditions present in nature, has motivated the study of convection in idealized settings where the fluid with a composition gradient is confined between two parallel horizontal plates and is heated from below. In this paper, we shall work with similar simplified setup because it conveniently brings forth the essential physics behind the phenomenon under study.

Let us consider a weakly-collisional dilute binary mixture plasma at rest confined between two horizontal parallel plates of infinite extent. The vertical separation between the plates is d and the acceleration due to gravity \mathbf{g} is acting vertically downwards. The bottom and the top boundaries are held at two different constant temperatures T_{bottom} and T_{top} respectively. The boundaries are also kept at constant concentrations (of, say, Helium ions) c_{bottom} and c_{top} , respectively. This sets up a constant background temperature gradient and a similar constant background concentration gradient in the confined plasma. Let there also be an externally imposed uniform magnetic field \mathbf{B} lying parallel to the vertical $x - z$ plane, without any loss of generality.

The equations of motion describing the dynamics (see also Pessah & Chakraborty (2013); Gupta et al. (2016)) of this system are given by

$$\frac{\partial \rho}{\partial t} + \nabla \cdot (\rho \mathbf{u}) = 0, \quad (1)$$

$$\frac{\partial \mathbf{u}}{\partial t} + \mathbf{u} \cdot \nabla \mathbf{u} = -\frac{1}{\rho} \nabla \cdot \left(\mathbf{P} + \frac{B^2}{8\pi} \mathbf{I} - \frac{B^2}{4\pi} \hat{\mathbf{b}} \hat{\mathbf{b}} \right) + \mathbf{g}, \quad (2)$$

$$\frac{\partial \mathbf{B}}{\partial t} = \nabla \times (\mathbf{u} \times \mathbf{B}) + \eta \nabla^2 \mathbf{B}, \quad (3)$$

$$\rho T \left(\frac{\partial s}{\partial t} + \mathbf{u} \cdot \nabla s \right) = (p_{\perp} - p_{\parallel}) \frac{d}{dt} \ln \frac{B}{\rho^{\gamma-1}} - \nabla \cdot \mathbf{Q}_s, \quad (4)$$

$$\frac{\partial c}{\partial t} + \mathbf{u} \cdot \nabla c = -\nabla \cdot \mathbf{Q}_c. \quad (5)$$

Here, the notations \mathbf{u} , ρ , T , s , γ and η stand for the fluid velocity, the density, the temperature (assumed to be the same for ions and electrons), the specific entropy, the adiabatic index, and the electrical resistivity (also called magnetic diffusivity) respectively. The pressure tensor (Hollweg 1985) is $\mathbf{P} \equiv p_{\perp} \mathbf{I} + (p_{\parallel} - p_{\perp}) \hat{\mathbf{b}} \hat{\mathbf{b}}$, where \mathbf{I} stands for the 3×3 identity matrix. The symbols \perp and \parallel refer respectively to the directions perpendicular and parallel to the magnetic field \mathbf{B} . Also, we have defined unit vector $\hat{\mathbf{b}} \equiv \mathbf{B}/B = (b_x, 0, b_z)$. The isotropic part of the pressure tensor — $P \equiv 2p_{\perp}/3 + p_{\parallel}/3$ — is assumed to satisfy the equation of state for an ideal gas

$$P = \frac{\rho k_B T}{\mu m_H}, \quad (6)$$

where k_B is the Boltzmann constant, μ is the mean molecular weight, and m_H is the atomic mass unit. Note that this equation of state implies $\alpha T = \alpha_{\mu} \mu = 1$, where $\alpha \equiv -(\partial \ln \rho / \partial T)_{P, \mu}$ and $\alpha_{\mu} \equiv (\partial \ln \rho / \partial \mu)_{P, T}$ are respectively the coefficient of thermal expansion and the coefficient of expansion due to change in mean molecular weight. The concentration c is related to μ as follows:

$$\mu = \left[(1 - c) \frac{1 + Z_1}{\mu_1} + c \frac{1 + Z_2}{\mu_2} \right]^{-1}. \quad (7)$$

Here Z_i and μ_i ($i \in \{1, 2\}$) are respectively the atomic number and the molecular weight of the i th ion. In our case, $i = 1$ for Hydrogen and $i = 2$ for Helium.

The anisotropic component of the pressure tensor in the momentum equation gives rise to Braginskii viscosity which is related to the coefficient of kinematic viscosity, ν . Also, $\mathbf{Q}_s \equiv -\chi \hat{\mathbf{b}} (\hat{\mathbf{b}} \cdot \nabla) T$, where χ is the thermal conductivity predominately due to electrons with $\chi \approx 6 \times 10^{-7} T^{5/2} \text{ erg cm}^{-1} \text{ s}^{-1} \text{ K}^{-1}$ (Spitzer 1962; Braginskii 1965). For later usage, we define coefficient of thermal diffusion $\lambda \equiv \chi / \rho c_p$, where $c_p \equiv T(\partial s / \partial T)_P$ is the heat capacity at constant pressure. Similarly, the composition of fluid elements changes due to change in the flux of the particles, $\mathbf{Q}_c \equiv -D \hat{\mathbf{b}} (\hat{\mathbf{b}} \cdot \nabla) c$, where D is the coefficient of the particle diffusion. In the equilibrium state, all the particles in the plasma are assumed to be described by a Maxwellian distribution with the same temperature, so that $p_{\parallel} = p_{\perp}$ initially. In general, the background heat (and particle) flux does not vanish, i.e., $\hat{\mathbf{b}} \cdot \nabla T \neq 0$ (and $\hat{\mathbf{b}} \cdot \nabla c \neq 0$), unless the magnetic field and the background gradients are orthogonal. The existence of a well-defined steady state, i.e., $\nabla \cdot \mathbf{Q}_s = 0$ (and $\nabla \cdot \mathbf{Q}_c = 0$), demands that the background temperature (and concentration) should be at most a linear function of the distance along the direction of the magnetic field. It has, thus, been implicitly assumed that the coefficients χ and D are constants that is justified under the local approximation that is used in the paper. This assumption is relaxed in, e.g., Latter & Kunz (2012); Kunz et al. (2012); Berlok & Pessah (2016).

Also, the sound crossing time associated with the modes of interest is much shorter than the growth rate of the unstable convective modes, it is justified to work within the Boussinesq approximation (Balbus 2000, 2001; Quataert 2008; Pessah & Chakraborty 2013; Gupta et al. 2016). Mathematically speaking, equation (1) thus reduces to

$$\nabla \cdot \mathbf{u} = 0. \quad (8)$$

In practice, under the Boussinesq approximation (Chandrasekhar 1981), the density variations can be mostly ignored except when it appears multiplied with the external gravity term.

The initial equilibrium state $(\mathbf{u}_*, \rho_*, P_*, T_*, c_*, \mathbf{B}_*)$ is defined by the following relations

$$\mathbf{u}_* = 0, \quad (9)$$

$$\frac{dP_*}{dz} \approx \frac{d(p_\perp)_*}{dz} = -\rho_* g, \quad (10)$$

$$T_* = T_{\text{bottom}} - \Delta T \left(\frac{z}{d} \right), \quad (11)$$

$$c_* = c_{\text{bottom}} - \Delta c \left(\frac{z}{d} \right), \quad (12)$$

$$\mathbf{B}_* = B_* \hat{\mathbf{b}} = B_*(\sin \phi \hat{\mathbf{x}} + \cos \phi \hat{\mathbf{z}}), \quad (13)$$

where $\Delta T \equiv T_{\text{bottom}} - T_{\text{top}}$, $\Delta c \equiv c_{\text{bottom}} - c_{\text{top}}$, and ϕ is angle between the uniform magnetic field and z -axis. We assume that the ion and electron pressures satisfy $P_i = P_e = P/2$. It is of use to recall that the plasma-beta parameter is defined as $\beta \equiv P_i/(B^2/8\pi)$. Henceforth, we omit the asterisk subscripts while denoting the equilibrium state.

3 LINEARISED EQUATIONS FOR PERTURBATIONS

Now we are fully equipped to find the dynamical equations for the infinitesimal perturbations about the equilibrium state. Owing to the Boussinesq approximation, the velocity field perturbation satisfy $\nabla \cdot \delta \mathbf{u} = 0$. Additionally one has, due to the solenoidal character of the magnetic field fluctuations, $\nabla \cdot \delta \mathbf{B} = 0$. Therefore, it suffices to understand the dynamics of only two independent components for both the velocity and the magnetic field components. They may be conveniently chosen as variables $\delta u_z, \delta \omega_z, \delta B_z$, and δj_z . Here

$$\delta \omega_z \equiv \partial_x \delta u_y - \partial_y \delta u_x, \quad (14)$$

$$\delta j_z \equiv \partial_x \delta B_y - \partial_y \delta B_x, \quad (15)$$

stand for the z -component of the fluctuations in the vorticity and the current density (times 4π), respectively.

It is convenient to use the characteristic scales in the problem in order to define a set of dimensionless coordinates according to $\mathbf{x}' \equiv \mathbf{x}/d$ and $t' \equiv t\nu/d^2$. Accordingly we define a set of dimensionless functions for all the dynamical variables of interest, i.e., $\delta u'_z \equiv \delta u_z d/\lambda$, $\delta \omega'_z \equiv \delta \omega_z d^2/\lambda$, $\delta B'_z \equiv \delta B_z/B$, $\delta j'_z \equiv \delta j_z d/B$, $\delta \theta' \equiv \delta T/\Delta T$, and $\delta c' \equiv \delta c/\Delta c$, such that

$$\delta f'(\mathbf{x}', t') \equiv \sum_{\mathbf{k}'} \hat{f}'(\mathbf{z}') \exp(i\mathbf{k}' \cdot \mathbf{x}' + \sigma' t'). \quad (16)$$

where f represents any of the aforementioned variables. The hat-symbol “ $\hat{}$ ” denotes the z -dependent Fourier transform amplitudes of the various functions involved, that are assumed to be periodic in the plane perpendicular to z . The dimensionless growth-rate (or frequency) σ' quantifies the exponential growth or decay of the perturbation with dimensionless wave vector $\mathbf{k}' = (k'_x, k'_y, 0)$. For the sake of brevity, in what follows, unless otherwise specified, we drop all the primes labeling dimensionless coordinates, variables, and functions. We also drop the hat-symbol denoting the Fourier amplitude of a given mode.

Taking the Laplacian of the z -component of momentum equation (2) and the z -component of its curl, we arrive at the following

equations of motion for δu_z and $\delta \omega_z$:

$$\left[\sigma(\partial_z^2 - k^2) - \frac{3}{k^2} (i \sin \phi k_x + \cos \phi \partial_z)^2 \times \right. \quad (17)$$

$$\left. (\cos \phi k^2 + i \sin \phi k_x \partial_z)^2 \right] \delta u_z = -R_T k^2 \delta \theta + R_c k^2 \delta c + Q \frac{P_r}{P_m} (i \sin \phi k_x + \cos \phi \partial_z) (\partial_z^2 - k^2) \delta B_z + \left[\frac{3i \sin \phi k_y}{k^2} (i \sin \phi k_x + \cos \phi \partial_z)^2 (\cos \phi k^2 + i \sin \phi k_x \partial_z) \right] \delta \omega_z,$$

$$\left[\left(\frac{3 \sin^2 \phi k_y^2}{k^2} \right) (i \sin \phi k_x + \cos \phi \partial_z)^2 \right] \delta \omega_z + \sigma \delta \omega_z = \quad (18)$$

$$+ Q \frac{P_r}{P_m} (i \sin \phi k_x + \cos \phi \partial_z) \delta j_z + \left[\frac{3i \sin \phi k_y}{k^2} (i \sin \phi k_x + \cos \phi \partial_z)^2 (\cos \phi k^2 + i \sin \phi k_x \partial_z) \right] \delta u_z.$$

Here, we have defined the following non-dimensional numbers: Rayleigh number (based on T) $R_T \equiv \alpha(\Delta T)gd^3/\lambda\nu$, Rayleigh number (based on c) $R_c \equiv \alpha_c(\Delta c)gd^3/\lambda\nu$, Chandrasekhar number $Q \equiv B^2 d^2/4\pi\rho\nu\eta$, Prandtl number $P_r \equiv \nu/\lambda$, and Magnetic Prandtl number $P_m \equiv \nu/\eta$. Following a similar procedure for induction equation (3), we obtain the equations for δB_z and δj_z ,

$$(\partial_z^2 - k^2 - P_m \sigma) \delta B_z = -\frac{P_m}{P_r} (i \sin \phi k_x + \cos \phi \partial_z) \delta u_z, \quad (19)$$

$$(\partial_z^2 - k^2 - P_m \sigma) \delta j_z = -\frac{P_m}{P_r} (i \sin \phi k_x + \cos \phi \partial_z) \delta \omega_z. \quad (20)$$

Similarly, we obtain the equation for the thermal fluctuations from equation (4) as

$$(\cos^2 \phi \partial_z^2 + 2i \sin \phi \cos \phi k_x \partial_z - \sin^2 \phi k_x^2 - P_r \sigma) \delta \theta \quad (21)$$

$$= \Sigma \delta u_z + \frac{1}{k^2} \left[(A_1 - A_2) k_x k_y + i A_5 k_y \partial_z \right] \delta j_z + \left[-\frac{A_1}{k^2} \partial_z - \frac{A_2}{k^2} k_x^2 \partial_z + A_3 \partial_z + i A_4 k_x + i \frac{A_5}{k^2} k_x \partial_z^2 \right] \delta B_z,$$

where we have used Schwarzschild number $\Sigma \equiv g\alpha T d/c_p \Delta T - 1$. Lastly, we also have

$$\left[\Lambda (\cos^2 \phi \partial_z^2 + 2i \sin \phi \cos \phi k_x \partial_z - \sin^2 \phi k_x^2) - P_r \sigma \right] \delta c \quad (22)$$

$$= -\delta u_z + \frac{\Lambda}{k^2} \left[(A_1 - A_2) k_x k_y + i A_5 k_y \partial_z \right] \delta j_z +$$

$$\Lambda \left[-\frac{A_1}{k^2} \partial_z - \frac{A_2}{k^2} k_x^2 \partial_z + A_3 \partial_z + i A_4 k_x + i \frac{A_5}{k^2} k_x \partial_z^2 \right] \delta B_z.$$

Here, $\Lambda \equiv D/\lambda$. In the preceding equations, we have used the notations: $A_1 \equiv \cos \phi$, $A_2 \equiv \cos \phi (\cos^2 \phi - \sin^2 \phi)$, $A_3 \equiv 2 \sin^2 \phi \cos \phi$, $A_4 \equiv \sin \phi (\sin^2 \phi - \cos^2 \phi)$, $A_5 \equiv -2 \sin \phi \cos^2 \phi$.

4 HELIUM FINGERS

The underlying concept of double diffusive convection is most easily intuited in the absence of any magnetic field and conductivity: Consider “warm salty over cold fresh” configuration, i.e., suppose saline water have the positive vertical gradients of both the temperature T and the salinity S , but is stably stratified in the sense that the vertical density gradient is negative. In this configuration, had the diffusive effects been absent, a blob of fluid is displaced vertically downwards would experience an upward buoyancy force because the density of its surrounding is more than the blob’s. However,

under the influence of diffusive processes, the situation becomes different. Since the heat diffuses much faster (by about 100 times) than the salt, the downwardly displaced blob of fluid can come in the thermal equilibrium with its surrounding while remaining more salty than the immediate surrounding. Thus, the blob may become denser than the surrounding and continue to fall under gravity giving way to the salt finger instability. This regime of the double diffusive convection is called the finger regime. As usual, the most basic techniques of linear stability analysis yield a dispersion relation implicitly relating the growth rate of a mode with its corresponding (horizontal) wave number. The inverse of the horizontal wave number associated with the fastest growth rate naturally corresponds to the width of the dominant salt fingers observed. While near the onset (critical condition) of the instability the convective cells' width is equal to the system height, in supercritical condition, one can derive (Stern 1960) an expression for the width W of the convection cell (salt finger) for the fastest growing mode as,

$$W = \left[\frac{g \left(\alpha_T \frac{dT}{dz} - \alpha_S \frac{dS}{dz} \right)}{\nu \lambda} \right]^{-1/4}. \quad (23)$$

Here, λ is heat diffusion coefficient, ν is kinematic viscosity, $\alpha_T = -(\partial \ln \rho / \partial T)_{P,S}$ is thermal expansion coefficient, $\alpha_S = (\partial \ln \rho / \partial S)_{P,T}$ is expansion coefficient due to salinity. It is in the supercritical regime that the convective cells become elongated and can now be aptly called salt finger. Note that for the constant temperature and the constant salinity gradients, the width $W \propto d^{1/4}$ where d is the system height.

When the magnetic field and, as is relevant in our case, the magnetic field driven anisotropic transport properties comes into effect, the situation is way more complicated both analytically and physically. Anyhow, our goal is to investigate the finger regime in the inner region of the ICM as modelled in this paper. This essentially means that we want to study the Helium fingers in the supercritical regime of the HBI modified by the concentration gradient. In fact, it can be shown (see Appendix A) that a typical ICM being observed now-a-days may be in supercritical state. All one has to do is to compare $d \ln(T/\mu)/dz$ in the ICM with the corresponding critical value of the gradient at which instability ensues or rather marginal state is attained. This critical value calculated using the convenient conducting stress-free boundary conditions and including the effect of magnetic tension is

$$\left. \frac{d}{dz} \ln(T/\mu) \right|_{\text{critical}} \approx \left(\frac{\pi^2}{\beta d} \right). \quad (24)$$

For an estimate, it may be noted that the critical value of $d \ln(T/\mu)/dz \approx 10^{-23} - 10^{-25} \text{ cm}^{-1}$ on using $\beta \approx 100 - 1000$ and $d = 10 - 100 \text{ kpc}$ for a typical inner region of galaxy cluster. However, on using the plot in Figure 5 of Pessah & Chakraborty (2013) based on Vikhlinin et al. (2006) and Bulbul et al. (2011), we may take $T_{\text{top}}=7.0 \text{ keV}$, $T_{\text{bottom}}=3.8 \text{ keV}$, $\mu_{\text{top}}=0.83$, $\mu_{\text{bottom}}=0.75$, and $d=50 \text{ kpc}$. Thus, from the fiducial profiles of the temperature and the mean-molecular weight, we find that the observed typical value of $d \ln(T/\mu)/dz \approx 10^{-23} \text{ cm}^{-1}$. This value evidently can be higher than the critical value. This means that a typical ICM being observed now-a-days may actually be in a supercritical regime when modelled as a fluid system undergoing double diffusive convection. This gives us hint that Helium fingers may be present in such ICMs.

In principle, our aforementioned endeavor of investigating the finger regime is straightforward. First, we have to find the mode

corresponding to the horizontal wave number $k = k_f$ (say) for which growth rate is fastest. Then, the width W_{He} of the Helium finger can be determined by putting equal to $2\pi/k_f$. We again want the dependence of the finger width on the height of the system. So, we have to choose the expression $g[\alpha(dT/dz) - \alpha_c(dc/dz)]/\nu\lambda$ — henceforth denoted as ξ for the sake of convenience — analogous to the salt finger case. Here, $\alpha_c \equiv (\partial \ln \rho / \partial c)_{P,T}$. Finally, we ask on which power of ξ the width of the finger depends. In other words, is there a value of $a \in \mathbb{R}$ for which a power-law relation of the following form

$$W_{\text{He}} = \left[\frac{g \left(\alpha \frac{dT}{dz} - \alpha_c \frac{dc}{dz} \right)}{\nu \lambda} \right]^a = \xi^a \quad (25)$$

is satisfied? It may be noted that for the constant temperature gradient and the constant concentration gradient, the width $W_{\text{He}} \propto d^{-a}$.

In order to put the idea into practice, we explicitly derive the following relevant dispersion relation by assuming the perturbation of the form $\sin(\pi z) e^{i(k_x x + k_y y) + \sigma t}$ and putting $\phi = 0$ in equations (17) to (22):

$$b_4 \sigma^4 + b_3 \sigma^3 + b_2 \sigma^2 + b_1 \sigma + b_0 = 0. \quad (26)$$

Here,

$$b_4 = (k^2 + \pi^2) P_m P_r^2, \quad (27)$$

$$b_3 = (1 + \Lambda) (k^2 + \pi^2) \pi^2 P_m P_r + (k^2 + \pi^2)^2 P_r^2 - 3k^2 \pi^2 P_m P_r^2, \quad (28)$$

$$b_2 = \pi^4 (k^2 + \pi^2) \Lambda P_m + (k^2 + \pi^2)^2 \pi^2 (1 + \Lambda) P_r - 3k^2 \pi^4 (1 + \Lambda) P_m P_r - 3k^2 \pi^2 (k^2 + \pi^2) P_r^2 + \pi^2 (k^2 + \pi^2) P_r^2 Q + k^2 P_m P_r (R_c + R_T \Sigma \Lambda), \quad (29)$$

$$b_1 = (k^2 + \pi^2)^2 \pi^4 \Lambda - 3k^2 \pi^6 \Lambda P_m - 3k^2 \pi^4 (k^2 + \pi^2) P_r (1 + \Lambda) + (k^2 + \pi^2) (1 + \Lambda) \pi^4 P_r Q + k^2 \pi^2 P_m R_T (1 + \Lambda \Sigma) + k^2 (k^2 + \pi^2) P_r (R_c + R_T \Sigma), \quad (30)$$

$$b_0 = -3k^2 \pi^6 \Lambda (k^2 + \pi^2) + \pi^6 (k^2 + \pi^2) \Lambda Q + k^2 \pi^2 (k^2 + \pi^2) R_c + \frac{k^2 \pi^4 P_m (\Lambda R_T - R_c)}{P_r} + k^2 \pi^2 (k^2 + \pi^2) \Lambda R_T \Sigma. \quad (31)$$

Then we solve for σ from this dispersion relation and plot the largest real part of growth rate, denoted as $[\text{Re}(\sigma)]_{\text{max}}$, versus k as depicted in Figure 1(a). We reiterate that we are interested in the inner region of the galaxy cluster, because the inner region of the galaxy cluster has the temperature and the concentration gradients as positive which is analogous to what happens in a salt finger system, and hence we choose the system parameters appropriately as given in the figure caption. We should also recall that we are dealing with non-dimensionalized quantities for which the unit of distance is d and that of time is d/ν^2 . For our case, these units explicitly are $d = 5 \times 10^{22} \text{ cm}$ and $d/\nu^2 = 25 \times 10^{18} \text{ s}$ respectively. Additionally, it should be noted that our results are concerned with the local modes in fluid limit as they should since the typical Knudsen number (ratio of ionic mean free path to the scale height) in the inner region of cool-core cluster is of the order of 10^{-3} (Kunz 2011; Pessah & Chakraborty 2013).

We note that $[\text{Re}(\sigma)]_{\text{max}}$ increases monotonically with k and $[\text{Re}(\sigma)]_{\text{max}}$ corresponds to the wave number $k = k_f = \infty$. This is consistent with the fact that the lowest mode first go unstable at k_f as detailed in the preceding paragraphs. This is not only inconvenient to work with but also is not physically allowed within the scope of our calculations: in our analysis, it doesn't make sense

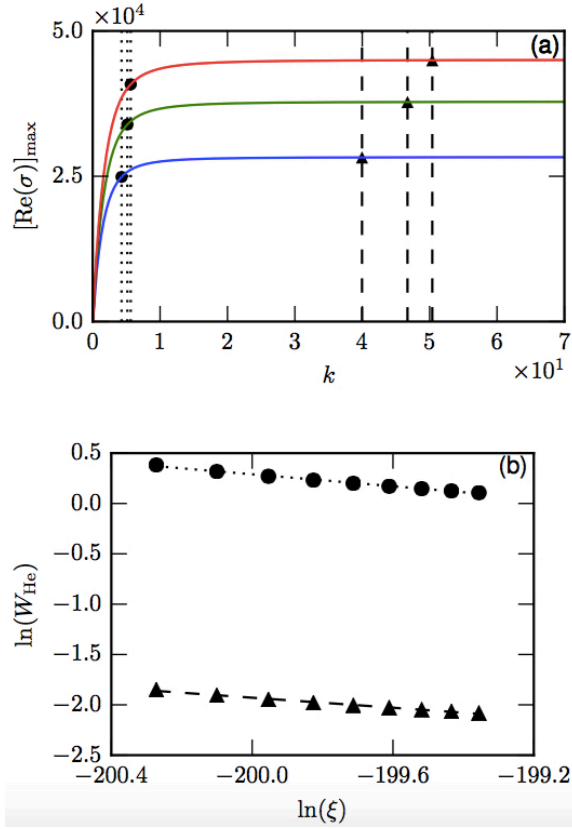


Figure 1. Width of the Helium fingers follows power law scaling. Upper panel (a) illustrates the largest real part of the growth rate, $[\text{Re}(\sigma)]_{\text{max}}$, as a function of horizontal wavenumber k for three different values of ξ fixed by choosing $\Delta T = -6 \times 10^6$ K (lower blue curve), $\Delta T = -8 \times 10^6$ K (middle green curve), and $\Delta T = -10^7$ K (upper red curve). The dotted lines and the dashed lines mark the corresponding $[\text{Re}(\sigma)]_{\text{max}}$ for k at which $d[\text{Re}(\sigma)]_{\text{max}}/dk$ equals 1250 and 2.5 respectively. Subsequently, we choose 9 different values of ΔT equispaced between -10^7 and -5×10^6 K, and hence 9 different values of ξ . Using these values of ξ , lower panel (b) exhibits two plots of $\ln(W_{\text{He}})$ vs. $\ln(\xi)$ — one for $d[\text{Re}(\sigma)]_{\text{max}}/dk = 1250$ (circles) and another for $d[\text{Re}(\sigma)]_{\text{max}}/dk = 2.5$ (triangles). The dotted line of slope -0.30 and the dashed line of slope -0.25 are the respective best fit lines. In plotting these curves, we have used $\nu = 10^{26} \text{ cm}^2 \text{ s}^{-1}$, $B = 2 \times 10^{-6}$ G, $\rho = 10^{-26} \text{ gm cm}^{-3}$, $d = 5 \times 10^{22} \text{ cm}$, $\Delta c = -0.2$, $c = 0.6$, and $\eta = 100 \text{ cm}^2 \text{ s}^{-1}$.

to choose a k that is larger than the inverse of the mean free path of the ions in the ICM, otherwise we are no longer in the fluid limit for the system under consideration. In order to bypass this issue, we use the fact that the curve of $[\text{Re}(\sigma)]_{\text{max}}$ vs. k (ξ fixed) is monotonic and appear to be saturating with k . We choose that k_f as k for which $d[\text{Re}(\sigma)]_{\text{max}}/dk$ is small, say, 1250. This value is chosen so that at this value the curve enters into the region where $d[\text{Re}(\sigma)]_{\text{max}}/dk$ no longer changes appreciably. Of course, strictly speaking this k_f does not correspond to the fastest growing perturbation. In Figure 1(a), we have plotted $[\text{Re}(\sigma)]_{\text{max}}$ with the horizontal wave number k for different values of ξ by varying the temperature difference between the two plates confining the plasma. We then choose k_f for each curve and thence find the corresponding Helium finger widths, W_{He} . Consequently, $\ln(W_{\text{He}})$ vs. $\ln(\xi)$ can be plotted (see Figure 1(b)) and from the slope of the resulting curve,

we can get the value of a . We, intriguingly, have found $a \approx -0.30$, very close to that is obtained for salt fingers (see equation 23).

In passing, we must make it clear that, in principle, one should have strictly worked with the fastest growing mode but that is not appropriate as discussed in the preceding paragraph. Instead we have used somewhat ad hoc modes and investigated its growth. This means that the power law exponent a is prone to modification in a realistic ICM, e.g., when we select $d[\text{Re}(\sigma)]_{\text{max}}/dk = 2.5$ which corresponds to k_f s greater than the ones obtained for $d[\text{Re}(\sigma)]_{\text{max}}/dk = 1250$, we get $a = -0.25$ that is even more close (within curve-fitting errors) to $-1/4$. Nevertheless, numerical simulations (see Figure 7 in Berlok & Pessah (2016)) validates the existence of thin Helium fingers. These fingers are observed en route to the turbulence state of the ICM.

5 DISCUSSIONS AND CONCLUSIONS

In this paper, we have applied the formalism usually employed for studying salt finger instability to investigate analogous convective instabilities in the inhomogeneous ICM. This approach goes beyond the standard linear mode analysis and has been carried out (however see Latter & Kunz 2012) by explicitly accounting for the boundary conditions commonly employed in the numerical simulations. Our work facilitates analytical understanding of some hitherto unexplored aspects of the dynamics of these instabilities. Moreover, in principle, this formalism is generalizable to address more realistic physical settings that, e.g., includes the effects of cosmic-rays (Chandran & Dennis 2006), radiative cooling (Balbus & Reynolds 2010; Latter & Kunz 2012), shear (Ren et al. 2011), rotation (Nipoti & Posti 2014), etc.

As far as the stability analyses of such inhomogeneous ICM modelled as weakly collisional dilute binary mixture of ions are concerned (Pessah & Chakraborty 2013; Berlok & Pessah 2015, 2016), for the first time we have an exact analytical expression for the stability criterion (equation (24)) that takes into account the effect of the magnetic tension. This analytical expression till now could not be arrived at using more widely employed and less cumbersome WKB-type perturbative methods (Balbus 2001; Quataert 2008; Pessah & Chakraborty 2013; Berlok & Pessah 2015). However, it must be acknowledged that the criterion in principle could be obtained numerically and that the magnetic tension has quantitative effect on the stability criterion can easily be seen within the WKB-formalism. Anyhow, using this result, we have deduced that many cool-core galaxy clusters may be in the supercritical regime and hence there is the possibility of existence of Helium fingers in the inner region of the ICMs. This is exactly what we have logically argued in this paper. Moreover, analogous to the finger regime of double diffusive instabilities in the absence of the magnetic field, the Helium fingers' width goes approximately as one-fourth power of the separation between the plates holding the fluid in the presence of vertical magnetic field — this is the main result of the paper. This intuitively makes sense simply because, as the Helium fingers are developing vertically downwards, the motion is along the magnetic field and hence the magnetic field is not presenting any obstruction to it via the Lorenz force. We remark that, as discussed earlier, even though the exact value of the exponent may not be robust, the power-law nature may still be. However, it is encouraging to note that the power law exponent a approaches $-1/4$ as one chooses larger value for k_f ; this fact is compatible with the aforementioned intuition.

This, however, may not be the case if the magnetic field is taken to be horizontal. We know that under the assumption of homogeneous ICM this case is more relevant in the outer region of ICM where the gradient of the temperature is typically negative giving rise to the MTI. Interestingly, there composition gradient could also be negative. This is reminiscent of diffusive regime (Kundu et al. 2012) of double diffusive instabilities leading to oscillatory instability in the corresponding saline water. Such oscillatory instability eventually results in the formation of a number of horizontal convecting layers. Analogously, thus, we expect similar horizontal convecting layers in the outer region of the ICM but of course the effect of the magnetic field could be significant. This issue of subtle interplay between the magnetic field and the flow patterns is worth pursuing as a future research direction.

Before we end, it must be admitted that the idealized setup of inhomogeneous plasma between two fixed plates along with the simplified boundary conditions, we have worked with in this paper can not be the complete picture of the ICM. Nevertheless, we have seen that it allows us to shed light on some aspects of double diffusive convection processes — generalization of the HBI and the MTI in the presence of the composition gradient — that play important role in the dynamics of the ICM. Some of the more positives of this particularly simple yet insightful setup could be as follows: Firstly, this approach provides a practical platform to make connections with numerical simulations because the boundary conditions usually adopted resemble the ones employed herein. Secondly, it identifies the critical value of the relevant gradients for the onset of the instabilities. Specifically, it can account for the effects of the magnetic tension on the stability criteria for both the HBI and the MTI. Thirdly, it provides an ideal platform for carrying out weakly nonlinear stability analysis for the convective instabilities. However, such an not-so-easy analysis is infested with subtle caveats and technicalities. Last but not the least, such analyses could enable invention of low dimensional models like the Lorenz model for Rayleigh–Bénard convection (Lorenz 1963; Chen & Price 2006) and magnetic Rayleigh–Bénard convection (Zierep 2003), capable of rendering further insights into the chaotic (turbulent) state of the ICM. As far as the choice of the boundary conditions are concerned, desire for analytical simplicity directed us to adopt conducting stress-free boundary conditions. They resemble those conveniently employed in numerical simulations. Of course, one could have worked with non-conducting stress-free, conducting rigid, non-conducting rigid, or some other possible boundary conditions but then it is not always possible to solve the corresponding problem analytically and even in the linear regime numerical techniques may become indispensable. Although, a particular choice of the boundary conditions is unlikely to have a drastic impact in the stability criterion within the bulk of the plasma, it must be realised that it may alter the detailed expression for the stability criterion.

ACKNOWLEDGEMENTS

We are thankful to Thomas Berlok, Martin E. Pessah, Shailendra K. Rathor, and Manohar K. Sharma for useful discussions. Part of this work was done during the visit of S. C. at TIFR Centre for Interdisciplinary Sciences, Hyderabad, India as a visiting faculty. S. C. acknowledges the financial support through the INSPIRE faculty award (DST/INSPIRE/04/2013/000365) conferred by the Indian National Science Academy (INSA) and the Department of Science and Technology (DST), India.

APPENDIX A: CRITERION FOR MARGINAL STATE IN HEAT- AND PARTICLE-FLUX-DRIVEN BUOYANCY INSTABILITY

In what follows, we exclusively adopt the reflective, stress-free, and perfectly conducting boundaries mathematically given by

$$\delta u_z(0) = \delta u_z(1) = 0, \quad (\text{A1})$$

$$\partial_z^2 \delta u_z(0) = \partial_z^2 \delta u_z(1) = 0, \quad (\text{A2})$$

$$\partial_z \delta \omega_z(0) = \partial_z \delta \omega_z(1) = 0, \quad (\text{A3})$$

$$\delta B_z(0) = \delta B_z(1) = 0, \quad (\text{A4})$$

$$\partial_z \delta j_z(0) = \partial_z \delta j_z(1) = 0, \quad (\text{A5})$$

$$\delta \theta(0) = \delta \theta(1) = 0, \quad (\text{A6})$$

$$\delta c(0) = \delta c(1) = 0. \quad (\text{A7})$$

Equation (A1) means that the normal component of the velocity is zero on the boundary surfaces. Equation (A2) and equation (A3) imply stress-free surfaces, whereas equation (A4) and equation (A5) model perfectly conducting boundaries. Equation (A6) and equation (A7) force the boundary surfaces to be at a constant temperature and concentration respectively. While facilitating analytically tractable calculations, this set of boundary conditions is also straightforwardly implementable in the numerical simulations.

Although in general $\phi \neq 0$, it is convenient to consider the case in which the magnetic field is along the z -direction, i.e., $\phi = 0$, that is known to be prone to the heat- and particle-flux-driven buoyancy instability (Pessah & Chakraborty 2013) which itself is the generalization of HBI in the presence of Helium concentration. This analytically tractable case is rich enough to make us appreciate the possible physical origin of the Helium fingers in the ICM. Hence, from now on we shall stick to this case.

In the state of marginal stability ($\sigma = 0$), the system of equation (17) and equation (18) are combined to give

$$\begin{aligned} & \left[-3k^2 \partial_z^4 + \left(\Sigma R_T + \frac{R_c}{\Lambda} \right) k^2 \right] (\partial_z^2 - k^2) \delta u_z = \\ & - \left[(R_T - R_c) \frac{P_m}{P_r} k^2 + Q(\partial_z^2 - k^2) \partial_z^2 \right] \partial_z^2 \delta u_z. \end{aligned} \quad (\text{A8})$$

Now, it is known that the dimensionless parameters Q and P_m have extremely large values in the ICM (Carilli & Taylor 2002; Peterson & Fabian 2006; Gupta et al. 2016). Thus, in this limit of interest, we may choose $Q, P_m \rightarrow \infty$, causing equation (A8) to reduce to

$$\left[(R_T - R_c) \frac{P_m}{P_r} k^2 + Q(\partial_z^2 - k^2) \partial_z^2 \right] \partial_z^2 \delta u_z = 0. \quad (\text{A9})$$

Now, the application of the chosen boundary conditions allows us to conclude (details are analogous to the calculations in Gupta et al. (2016)) that

$$\delta u_z = A \sin n\pi z, \quad (\text{A10})$$

(A being constant), along with

$$R_T - R_c = -n^2 \pi^2 \left[\frac{n^2 \pi^2 + k^2}{k^2} \right] Q \frac{P_r}{P_m}. \quad (\text{A11})$$

$$\Rightarrow \frac{d}{dz} \ln(T/\mu) = n^2 \pi^2 \left[\frac{n^2 \pi^2 + k^2}{k^2} \right] \left(\frac{1}{\beta d} \right). \quad (\text{A12})$$

Since the R.H.S. of equation (A12) is non-negative, the marginal state can exist when (i) ΔT is negative i.e., top plate is hotter and $\Delta \mu > 0$, or (ii) ΔT is positive (bottom plate hotter) and $\Delta \mu > 0$ but $|\Delta \ln T| < |\Delta \ln \mu|$, or (iii) $\Delta \mu$ and ΔT are both negative, i.e., top plate

is hotter and at higher concentration, such that $|\Delta \ln T| > |\Delta \ln \mu|$. The last case may be satisfied (in accordance with the Helium sedimentation model) in the inner region of the ICM in cool-core galaxy cluster. Here, the onset of instability happens for the lowest mode ($n = 1$) for the maximum value of $k = \infty$ at which $(\pi^2 + k^2)/k^2$ attains the minimum value 1. Therefore, the criterion for the onset of instability is

$$\left. \frac{d}{dz} \ln(T/\mu) \right|_{\text{critical}} \approx \left(\frac{\pi^2}{\beta d} \right), \quad (\text{A13})$$

The ‘equal to’ sign has not been put in this stability criterion because it must be kept in mind that in order to remain within the fluid limit, k can at most be of the order of inverse of the mean free path of the ions. Similar objection can be raised against the usage of $n = 1$ as it isn’t compatible with the local approximation; this however is not a very serious concern since choosing any larger value of n only modifies the constant multiplicative numerical factor in the R.H.S. of equation (A13). Most important aspect of the mathematical expression of the criterion is that it takes into account the effect of magnetic field strength (or equivalently the timescale of Alfvén velocity). Such an analytical expression is missing in the work done by Pessah & Chakraborty (2013); Berlok & Pessah (2015, 2016) and hence equation (A13) is a new result. It explicitly shows that the critical limit of the gradient of (T/μ) increases proportional to the square of the strength of the background magnetic field.

REFERENCES

- Abramopoulos F., Chanan G. A., Ku W. H.-M., 1981, *ApJ*, 248, 429
- Balbus S. A., 2000, *ApJ*, 534, 420
- Balbus S. A., 2001, *ApJ*, 562, 909
- Balbus S. A., Reynolds C. S., 2010, *ApJL*, 720, L97
- Berlok T., Pessah M. E., 2015, *ApJ*, 813, 22
- Berlok T., Pessah M. E., 2016, *ApJ*, 824, 32
- Braginskii S. I., 1965, *RvPP*, 1, 205
- Bulbul G. E., Hasler N., Bonamente M., Joy M., Marrone D., Miller A., Mroczkowski T., 2011, *A&A*, 533, A6
- Carilli C. L., Taylor G. B., 2002, *ARA&A*, 40, 319
- Chandran B. D., Dennis T. J., 2006, *ApJ*, 642, 140
- Chandrasekhar S., 1981, *Hydrodynamic and Hydromagnetic Stability*. Dover Publications, NY
- Charbonnel C., Zahn J.-P., 2007a, *A&A*, 476, L29
- Charbonnel C., Zahn J.-P., 2007b, *A&A*, 467, L15
- Chen Z. M., Price W. G., 2006, *CSF*, 28, 571
- Chuzhoy L., Loeb A., 2004, *MNRAS*, 349, L13
- Chuzhoy L., Nusser A., 2003, *MNRAS*, 342, L5
- Fabian A. C., Pringle J. E., 1977, *MNRAS*, 181, 5P
- Gupta H., Rathor S., Pessah M., Chakraborty S., 2016, *PhLA*, 380, 2407
- Hollweg J. V., 1985, *JGRA*, 90, 7620
- Kundu P. K., Cohen I. M., Dowling D. R., 2012, *Fluid Mechanics* (Fifth Edition). Academic Press
- Kunz M., 2011, *MNRAS*, 417, 602
- Kunz M. W., Bogdanović T., Reynolds C. S., Stone J. M., 2012, *ApJ*, 754, 122
- Kunze E., 1987, *JMR*, 45, 533
- Latter H. N., Kunz M. W., 2012, *MNRAS*, 423, 1964
- Lorenz E. N., 1963, *JAtS*, 20, 130
- McDougall T. J., 1981a, *PrOce*, 10, 71
- McDougall T. J., 1981b, *PrOce*, 10, 91
- Markevitch M., Vikhlinin A., 2007, *PhR*, 443, 1
- Monchick L., Mason E. A., 1967, *PhFl*, 10, 1377
- Mroczkowski T., 2011, *ApJL*, 728, L35
- Nipoti C., Posti L., 2014, *ApJ*, 792, 21
- Özgökmen M. T., E. E. O., 1998, *PhFl*, 10, 1882
- Peng F., Nagai D., 2009, *ApJ*, 693, 839
- Pessah M. E., Chakraborty S., 2013, *ApJ*, 764, 13
- Peterson J., Fabian A., 2006, *PhR*, 427, 1
- Qin B., Wu X.-P., 2000, *ApJL*, 529, L1
- Quataert E., 2008, *ApJ*, 673, 758
- Radko T., 2008, *JFM*, 609, 59
- Radko T., 2010, *JFM*, 645, 121
- Ren H., Cao J., Dong C., Wu Z., Chu P. K., 2011, *PhPl*, 18, 022110
- Rephaeli Y., 1978, *ApJ*, 225, 335
- Schmitt R. W., 1979, *DSRI*, 26, 23
- Shtykovskiy P., Gilfanov M., 2010, *MNRAS*, 401, 1360
- Spitzer L., 1962, *Physics of Fully Ionized Gases*. Wiley Interscience, New York
- Stern M. E., 1960, *Tell*, 12, 172
- Ulrich R. K., 1972, *ApJ*, 172, 165
- Vikhlinin A., Kravtsov A., Forman W., Jones C., Markevitch M., Murray S. S., Speybroeck L. V., 2006, *ApJ*, 640, 691
- Zierup J., 2003, *TAM*, pp 23–40